Engineering with Computers (2016) 32:231–246
DOI 10.1007/s00366-015-0412-3

ORIGINAL ARTICLE

Influence surfaces by boundary element/least square methods coupling

Valério da Silva Almeida[1] · **Luttgardes de Oliveira Neto**[2]

Received: 13 June 2014 / Accepted: 11 August 2015 / Published online: 2 September 2015

Abstract This work presents a new application for calculating the influence surfaces of transverse displacements, directional derivatives and bending moments for generic bridge decks. A plate bending boundary element method formulation is coupled with the application of a continuous field surface derived by the least square procedure. This original BE formulation permits calculating influence surfaces of plates with polygonal, curved or circular geometry, and several transverse load conditions. The proposal allows future analysis of building floors and single and continuous bridge trusses connected to longitudinal and transversal girders. Numerical examples are presented to demonstrate the potential of the present formulation and the results are compared with analytical values and with usual vehicular loads.

Keywords Influence surfaces · Thin plates · Boundary element method · Least square procedure

1 Introduction

In roadways and bridge decks, the variable moving vehicle loads must be considered for calculating stress, deflections, bending moment and shear force for the safe design of the structure. A referential vehicle is located in many positions to obtain the design variable envelopes, which are usually called influence surfaces for bi-dimensional analysis.

In this context, the thin plate theory is applied for this evaluation, in which some models have been developed along two distinct lines. In the first, manual methods were developed generating famous influence surface charts, which were obtained by solving the differential equations using Fourier series for various shapes and support conditions. In this category, Rusch and Hergenroder [30] and Rusch [31] approaches, and respectively charts, are currently applied in this line. One of the most famous design charts was produced by Pucher [28], who presented a collection of influence surface charts for isotropic slabs; British and American Standard Specifications use this method. However, these procedures are very cumbersome, and impossible in most cases, for solving plates with irregular geometries, non-conventional types of loadings, the presence of cavities, curved or skewed side plates, and do not allow internal support conditions. Besides, the bending moment and shear force obtained using these charts are very conservative.

The second line of research uses a powerful numerical method, such as the finite element method (FEM) for stress/strain calculation in conjunction with other mathematical tools. Some groups developed specific FE formulations for computing influence surfaces, such as Orakdogan and Girgin [23] and Shen [34] who presented generalizations of the classical Muller Breslau principle using Betti´s law to construct influence surfaces. Other researchers applied commercial FEM software integrated with some other procedures, such as Memari and West [20], who used the 3D FEM and the technique called ‘adjoint method’ for determining the influence surface, or Kong [17], who developed

✉ Luttgardes de Oliveira Neto
lutt@feb.unesp.br

Valério da Silva Almeida
valerio.almeida@usp.br

[1] Department of Structural and Foundation Engineering, School of Engineering of the University of São Paulo (EPUSP), São Paulo, SP, Brazil

[2] Department of Civil Engineering, Faculty of Engineering (FE), UNESP, Av. Eng. Luiz Edmundo Coube, 17033-360 Bauru, SP, Brazil

a practical method to determine critical moments of bridge decks using the method of least squares and spreadsheets with FE software.

In all the lines of work discussed so far, both procedures have some disadvantages for treating influence surface; the former ones are limited for general problems, and the latter, for simulating complex problems, makes it necessary to refine the discretization of the structure geometry, which requires huge computational work and the results have strong mesh dependencies.

In light of these considerations, this work presents a new application for calculating the influence surfaces of transverse displacements, directional derivatives and bending moments for bridge decks using the boundary element method (BEM) with the application of a continuous field surface derived from the least square procedure. Two works presented similar coupling proposal, with boundary method and least square (nodal) procedure applied to thin plates subjected to concentrated loads [37, 38].

The BEM has advantages over FEM when applied to analyze surface and volume bodies because the problems are formulated using boundary integrals, in which variables are calculated. In other words, the problems are formulated with one dimension less than the real problem. In elastic-linear problems, the internal discretization is not necessary, making it advantageous to determine influence surfaces of bending plates and, consequently, not requiring longer computational processing cost. Another advantage of using BEM over FEM is the non-domain mesh dependency of the former, an extremely important factor in accurately computing the design variables of the domain.

This formulation also allows calculating influence surfaces of plates with polygonal, curved or circular geometry, and a Gaussian coordinate transformation is used over the boundary elements to obtain internal values at points very close to the boundary with good results. The proposal permits future analysis of building floors and bridge trusses, simulating both isolated and continuous plates connected to longitudinal and transversal girders under normal traffic loads defined by specific standards. Numerical examples are presented to prove and to demonstrate the potential of the present formulation and the results are compared with analytical values.

2 Boundary element method

The BEM is already recognized as an alternative to the FEM when solving different engineering problems, but it is still necessary to optimize studies and formulations for new applications.

The direct method for elastic bending plates was elaborated by Hansen [14], followed by the studies by Bezine [6] and Stern [36], who, in turn, developed direct formulations based on Green identity, which considers two integral equations that are relative to the transverse displacement and its normal derivative to the boundary line. Afterwards, basic and pioneer studies were produced by Tottenham [40], Wu and Altiero [42], Hartmann and Zotemantel [15], Song and Mukherjee [35], Paris and Leon [27], Abdel-Akher and Hartley [2] and Beskos [5].

Very recent works have aimed to apply BEM formulations considering different aspects of civil engineering, such as stiffened plate by beams, shear deformation, plate over foundations and laminated plates, such as Almeida and Paiva [3, 4], Rashed [29], Sapountzakis and Mokos [32], Waidemam and Venturini [41], Fernandes [11], Shao and Wu [33], Hwu [16], Palermo Jr [26], or simulations such as damage, fracture, vibration or modal analysis, in which line we can cite Fudoli et al. [12], Botta et al. [7], Xia et al. [43], Citarella and Cricrì [8] and [9], Paiva et al. [25].

Considering several plate geometries, the analytical integral resolution for geometrically linear elements is possible, but solutions are difficult when the elements are geometrically curved. For bending plates, Oliveira Neto and Paiva [21] proved that the best solutions require an approximation by curved boundary elements (quadratic or circular). The same formulation is used here; the integral resolution is carried out numerically, a Gaussian coordinate transformation is used over the boundary elements and the equivalent shear forces, V_n, are represented as a concentrated force in the nodes of the boundary [21]. These propositions allow obtaining internal values at points very close to the boundary or to concentrated loads with good numerical precision.

2.1 Integral equations for bending plates

The integral equations for fixed and free-boundary plates involve the following boundary variables: transverse displacement w, directional derivative $\mathrm{d}w/\mathrm{d}n$, equivalent shear force V_n and normal bending moment m_n, and their respective fundamental solutions w^*, $\mathrm{d}w^*/\mathrm{d}n$, V_n^*, m_n^* (Fig. 1).

The integral Eq. (1) for the transverse displacement w and its directional derivative $\mathrm{d}w/\mathrm{d}n$ at point Q are written by means of the summation of boundary integrals, which are then performed on every boundary element, defined geometrically based on the nodal values:

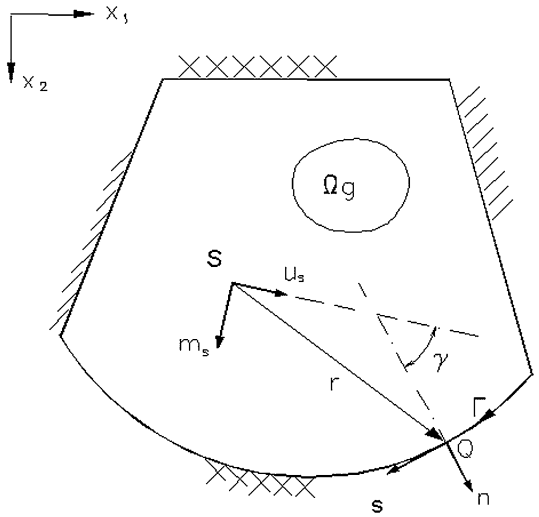

Fig. 1 Plate with load region Ω_g

$$C(Q)U(Q) + \sum_{l=1}^{Ne} \int_{-1}^{1} J_k \, \phi^k \, p^*(Q,P) \, U_k \, d\xi + \sum_{i=1}^{Nc} R^*_{c_i}(Q,P) \, U_{c_i}(P) = \sum_{l=1}^{Ne} \int_{-1}^{1} J_k \, \phi^k \, u^*(Q,P) \, P_k \, d\xi + \sum_{i=1}^{Nc} R_{c_i}(P) \, u^*_{c_i}(Q,P) + \int_{\Omega_g} g(p) \, u^*(Q,p) d \, \Omega_g(p) \quad (1)$$

in which, $C(Q) = \beta/2\pi$, with β as the internal angle of the boundary at point Q; $J^k = \frac{d\,\Gamma_l}{d\xi} = \sqrt{\left(\frac{dx}{d\xi}\right)^2 + \left(\frac{dy}{d\xi}\right)^2}$ is the Jacobean of the local coordinate transformation; $U_k^T = \left\{ w^1 \left(\frac{\partial w}{\partial n}\right)^1 w^2 \left(\frac{\partial w}{\partial n}\right)^2 w^3 \left(\frac{\partial w}{\partial n}\right)^3 \right\}$ is the boundary displacement vector; $P_k^T = \left\{ V_n^1 m_n^1 V_n^2 m_n^2 V_n^3 m_n^3 \right\}$ is the boundary bending moment and equivalent shear force vector; ϕ^k represents the interpolate function for boundary variables, quadratic polynomials are used in this formulation; R_c is the corner reaction; $R_c = m_{ns}^- - m_{ns}^+$ $u^{*T} = \left\{ w^*(Q,\, P) \left(\frac{\partial w^*}{\partial n}\right)(Q,\, P) \right\}$ is the fundamental displacement vector; $p^{*T} = \left\{ V_n^*(Q,\, P)\; m_n^*\,(Q,\, P) \right\}$ is the fundamental bending moment and equivalent shear force vector; and g(p) is the transverse load distributed over domain region Ω_g.

In BEM, the boundary is divided into elements whose variables are approximated by interpolate functions, preserving the continuity of displacement function along element boundaries.

In the cases that use quadratic or circular approximation, three points are necessary to geometrically define the boundary element, and the approximate functions are as follows:

$$\phi^1 = \frac{1}{2}\xi(\xi - 1); \quad \phi^2 = (1 - \xi)(1 + \xi); \quad \phi^3 = \frac{1}{2}\xi(\xi + 1)$$

in which ξ is a local non-dimensional coordinate.

The detailed expressions that define geometrically quadratic and circular elements are described in Oliveira Neto and Paiva [21].

Equation (1), written for all the boundary points, results in a system of linear equations as expressed in Eq. (2):

$$[\mathbf{H}]\{\mathbf{U}\} = [\mathbf{G}]\{\mathbf{P}\} + \{\mathbf{T}\} \quad (2)$$

in which [**H**] and [**G**] are matrices obtained by calculating boundary integrals over all boundary elements; {**T**} is the vector with contributions of transverse distributed load $g(p)$ over domain region Ω_g.

Imposing the boundary conditions, taking them to vector {**P**} and changing the correspondent columns of [**H**] and [**G**], the system of equations can be rewritten as:

$$[A]\{X\} = \{B\} \quad (3)$$

where {**X**} is the vector of the unknown nodal variables at the boundary, [**A**] has contributions from matrices [**H**] and [**G**] after changing columns.

2.2 Equations of bending moments on internal points

After the resolution of system (3), the unknown variables of the boundary are calculated and it is possible to obtain the displacements $w(s)$, the direction derivatives $\partial w/\partial m$ and the curvatures in relation to a direction m for the domain points. As such, the following matrix equation is obtained, similar to that already described for the boundary points:

$$\{U(s)\} + \left[H'\right]\{U\} = \left[G'\right]\{P\} + \left\{p'\right\} \quad (4)$$

where

$$\{U(s)\}^{\mathrm{T}} = \left\{ w_1 (\partial w/\partial m)_1 \ldots w_{\mathrm{Npi}} (\partial w/\partial m)_{\mathrm{Npi}} \right\}$$

being, N_{pi} the number of internal points.

In turn, the bending and twisting moments in the internal points are given by equations expressed in the indicated form:

$$M_{ij} = -D\left[\nu \delta_{ij} \frac{\partial^2 w}{\partial x_l \partial x_l} + (1 - \nu) \frac{\partial^2 w}{\partial x_i \partial x_j} \right], \quad \text{with, } i,j,l = 1,2 \quad (5)$$

Here D is the flexural rigidity and v is the Poisson's ratio. Replacing the integral equation of displacement w (4) at a plate domain point into the moment Eq. (5), and performing the necessary integrations, the integral equation of the bending moment of the plate domain points is obtained:

$$M_{ij}(s) = -\int_{\Gamma}\left[q^{*}_{n_{ij}}(s,Q)w(Q) - m^{*}_{n_{ij}}(s,Q)\frac{\partial w}{\partial n}(Q) - m^{*}_{ns_{ij}}(s,Q)\frac{\partial w}{\partial s}(Q)\right]d\Gamma(Q) + \int_{\Gamma}\left[V_n(Q)w^{*}_{ij}(s,Q) - m_n(Q)\frac{\partial w^{*}}{\partial n_{ij}}(s,Q)\right]d\Gamma(Q) + \sum_{c=1}^{N_c} R_c(Q)w^{*}_{c_{ij}}(S,Q) + \int_{\Omega_g} g(q)w^{*}_{ij}(S,q)d\Omega_g(q). \quad (6)$$

The algebraic equations of bending moments can be written by a similar procedure already described as:

$$\{\mathrm{M(s)}\} = -\left[\mathrm{H''}\right]\{\mathrm{U}\} + \left[\mathrm{G''}\right]\{\mathrm{P}\} + \left\{\mathrm{p''}\right\} \quad (7)$$

where $\{M(s)\}^{\mathrm{T}} = \{M_1 M_2 \cdots M_{\mathrm{Npi}}\}$, $\{M_i\}^{\mathrm{T}} = \{M_x M_{xy} M_y\}$ and M_x, M_y and M_{xy} are bending and twisting moments, defined, respectively, as $M_x = \int_{-h/2}^{h/2}\sigma_x z\mathrm{d}z$, $M_y = \int_{-h/2}^{h/2}\sigma_y z\mathrm{d}z$ and $M_{xy} = \int_{-h/2}^{h/2}\tau_{xy} z\mathrm{d}z$.

3 Influence surface determination

For calculating the maximum effect E_s at a defined cross section of a structural element by boundary element formulation, this effect depends on the summation of maximum effects at the same cross section as the result of loads applied to all points of the structural element. This way, the structure must be computed several times by a unitary load applied to those points to obtain the set of maximum effects E_s at the specified cross section.

Those discrete values are defined as required for each point and they will be computed to trace the influence surface of effect E_s at the defined cross section.

The direct use of the fundamental solution in determining the influence surface (IS) is most appropriate when one knows the position of the dead and/or standard vehicle loads. In case of determining the position of these critical actions to take to the extreme effect of E_s at a defined cross section of the structural element, the knowledge of a function that represents its IS, $\eta_s\ (x,\ y)$ is more suitable and reliable. For instance, consider the case of one-dimensional structure and the influence line (IL) of an effect E_s at defined cross section S (see Fig. 2a):

The determination of the positive extreme effect, E_S^{+}, of an effect E_s, is achieved by the known curve $\eta_s(x)$ and it is necessary to apply it as follows:

The distributed vehicle load (q), which has a variable length, must be applied over sections with values $\eta_s(x) > 0$ and concentrated loads of standard vehicle P_i positioned at coordinates $\eta_s(x) > 0$.

The determination of positive areas defined by IL ($A_{S_i}^{+}$) and the ordinate ($\eta_S^{+}(x)$) is not obvious as one might imagine. Even getting $\eta_s(x)$ at discrete positions, directly using the fundamental solution, the maximization of this effect (or minimization for the case of minimum effects E_S^{-}) leads to very inaccurate values due the inappropriate procedure for determining these areas and localizing the ordinates for all the concentrated loads and arranging them continuously for getting extremes effects.

What is the total area A_S^{+}? Where are the loads P_i applied to obtain the maximum/minimum effect?

The use of an adequately known function $\eta_s(x)$ facilitates this process since the optimization problem can be written as follows:

$$\left.\begin{matrix}\max(E_s)\\ \min(E_s)\end{matrix}\right\} = \int_{x_0}^{x_0+\mathrm{var}} q(x)\cdot\eta_s dx + \sum P_i\cdot\eta(x)$$

subject to

$$P(x) = \begin{cases} P_1(x) \\ P_2(x+a) \\ P_3(x+a+b)\end{cases} \quad and\ q(x) = q, (x_0 < x < x_0 + \mathrm{var.})$$

Similarly, it should be extended to the case of two-dimensional structure and influence surface, where the surfaces must be determined, its volume, and to which certain positions the loads must be applied (see Fig. 2b).

The determination of a known function surface $\eta_s(x,\ y)$ for effect E_s also facilitates this process, and we must thus determine the regions that generate extreme values by solving the following optimization problem:

$$\left.\begin{matrix}\max(E_s)\\ \min(E_s)\end{matrix}\right\} = \int_{\Omega} q(x,y)\cdot\eta_s(x,y)d\Omega \ + \ \Sigma P_i\cdot\eta(x,y)$$

subject to

$$P(x,y) = \begin{cases} P_1(x,y) \\ P_2(x+a,y) \\ P_3(x+a+b,y) \\ P_1(x,y-c) \\ P_2(x+a,y-c) \\ P_3(x+a+b,y-c)\end{cases} \quad and\ q(x,y) = q, (x_0 < x < x_0 + \mathrm{var.}), (y_0 < y < y_0 + d)$$

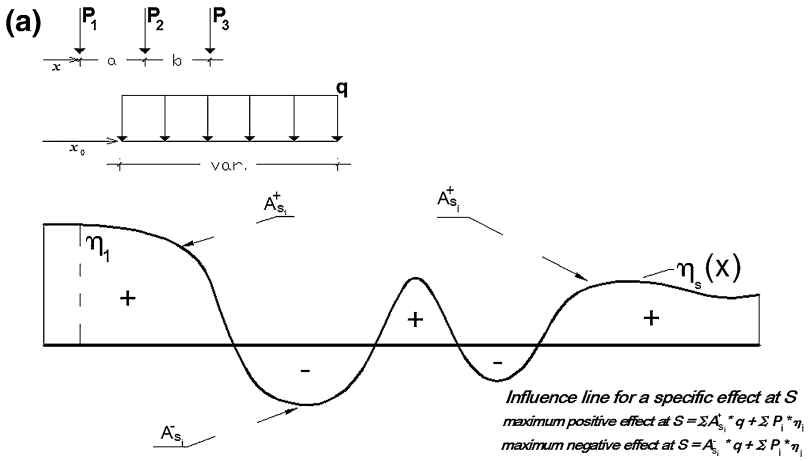

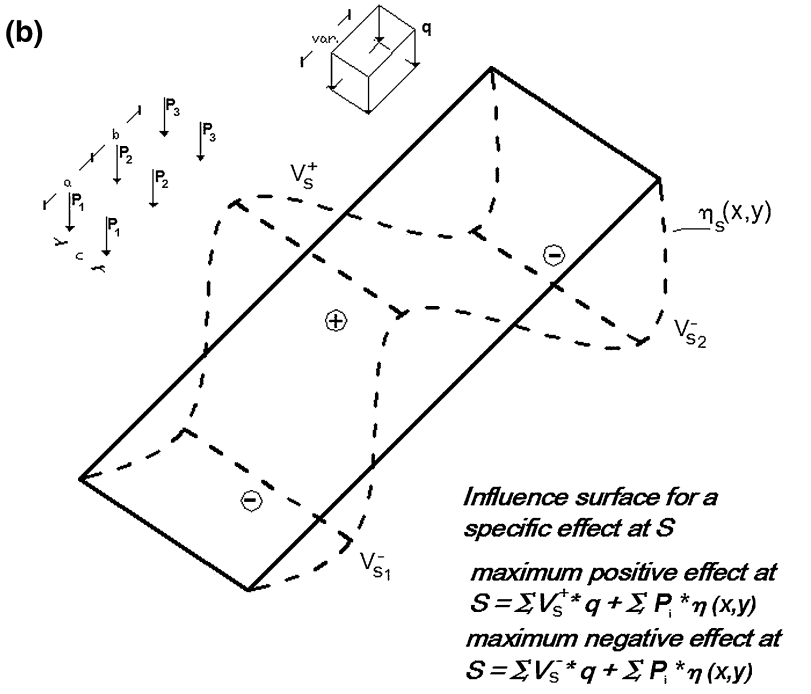

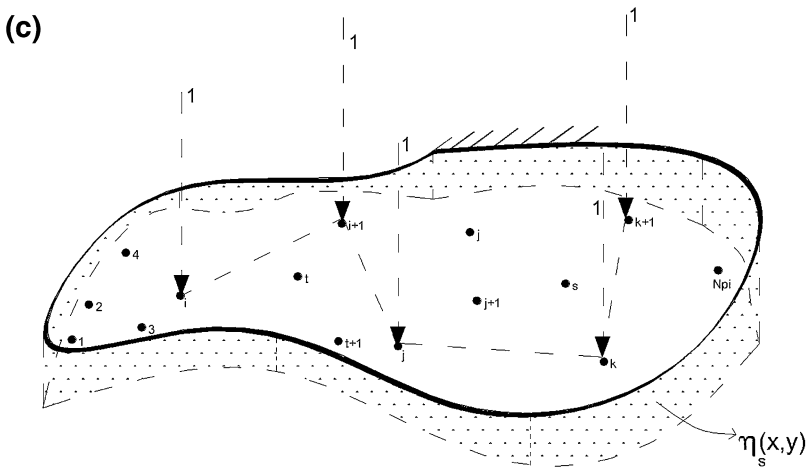

Fig. 2 **a** Concept for calculating maximum/minimum design effects subject to concentrated vehicle and distributed loads for beams. **b** Concept for calculating maximum/minimum design effects subject to concentrated vehicle and distributed loads for plates. **c** Influence surface of point *s* on the plate

Thus, both optimization problems with restrictions can be solved immediately using a classical deterministic process.

This optimization process is not applied herein to determine extreme actions. We made the generation of influence surfaces investigating and determining the parameters of their generation to bring the ordinate values and regions for the subsequent application of loads in the process of determining the extreme actions at a defined cross section of the structural element.

The study of vehicle loads initiates with the determination of the influence surface, $\eta_s(x, y)$. The numerical procedure starts with the plate discretization in boundary elements and the definition of a total of 'n' points inside, on which the unit load equivalent is applied. At each iteration, corresponding to the unit load positioned on each internal point "i", the boundary unknowns are determined by solving equation system (3). In the same iteration, after calculating the boundary values, Eqs. (4) and (7) are applied to obtain the internal displacements, moments and shear forces. All of these calculated values are stored in temporary individual files that must be used to generate the 'extreme quantity surfaces'.

For each type of response, a surface is generated with the extreme values at each internal point 'i' corresponding to the variation of the unitary load applied to all 'n' domain points. All of these calculated and stored values are used for generating 'influence surfaces', as shown in Fig. 2c. The 'influence surface', $\eta_s(x, y)$, refers to an effect Es that derives from a generic section 's' of domain Ω when an unitary load is applied to all the points regularly spread on the plate domain.

Note that the equivalent unit concentrated load is actually a uniformly distributed load over a small square region whose center is the chosen load point. Domain integrals $\int_{\Omega_g}$ in Eqs. (1), (4) and (6) are transformed into a summation of integrals over boundary Γ_g of each respective loaded region (Oliveira Neto and Paiva, [21]). This proposal permits the calculation of internal values, mainly bending moments, at load points avoiding strong singularities in fundamental solutions of these equations and high gradients in internal values, e.g., bending moments. This BE technique also justifies the use of the least square technique to fit the discrete values obtained by the procedure described. Even for small areas of plate support, such as plates supported on columns, there are no high gradients in bending moment values, as proved in Paiva and Venturini [24] and Oliveira Neto and Paiva [22].

3.1 Effect approximation discretized by the least square procedure

The extreme effects E_s are obtained in sections "s" of the domain and the boundary. Each of these effects can be represented by a continuous field surface with the application of a polynomial interpolation of the least square type.

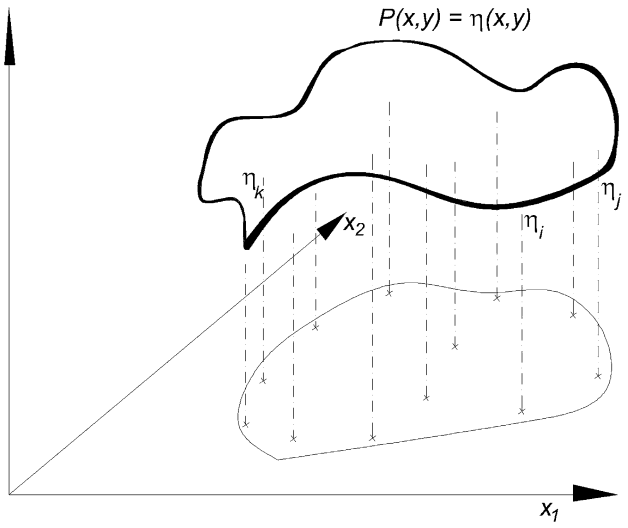

Fig. 3 Scheme of the tridimensional surface adjustment

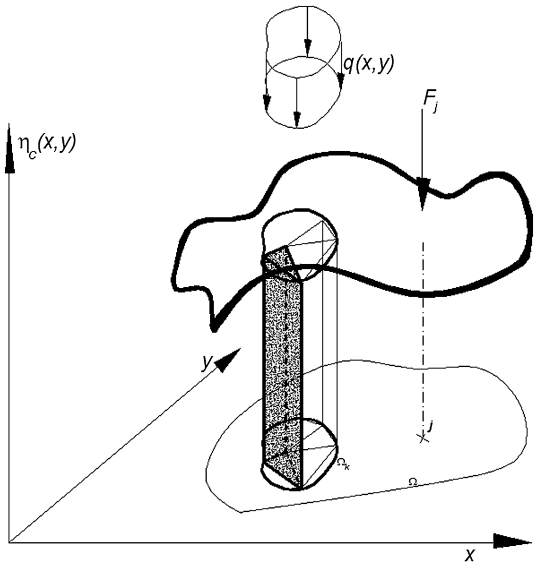

Fig. 4 Load effect determination (E_c) using numerical integration with the automated Delaunay triangulation

The surface adjustment by the least square method is a mathematical procedure for finding the best-fitting surface that adjusts to the set of values of a given sample, so as to minimize the square of the distance between this surface and these points [18].

A continuous field can be obtained using this adjustment procedure, producing a surface in terms of the defined values read in the domain and boundary, which can be displacements or bending moment values.

For the sake of simplicity and following the Weierstrass theory, it is possible to approximate the domain field by polynomial functions, and this procedure does not induce considerable numerical errors, provided the approximating fields do not have high gradient for displacement or bending moments at points of the domain. This occurs, for instance, in problems that consider fracture or damage mechanical theory, which is not considered herein.

domain, n indicates the total number of known values, or internal points.

Substituting the approximation of $\bar{\eta}(x,y)_k$ given by expression (8) in (11) and minimizing function Q in relation to each term of real coefficients, it arrives at a linear system with the polynomial coefficients of the unknown values. The matricial representation of this system is generically given by:

$$\begin{bmatrix} n & \sum_{i=1}^{n} x_i & \sum_{i=1}^{n} y_i & \sum_{i=1}^{n} x_i \cdot y_i & \sum_{i=1}^{n} x_i^2 & .. & .. & \sum_{i=1}^{n} y_i^m \\ \sum_{i=1}^{n} x_i & \sum_{i=1}^{n} x_i^2 & \sum_{i=1}^{n} x_i \cdot y_i & \sum_{i=1}^{n} x_i^2 \cdot y_i & \sum_{i=1}^{n} x_i^3 & .. & .. & \sum_{i=1}^{n} x_i \cdot y_i^m \\ \sum_{i=1}^{n} y_i & \sum_{i=1}^{n} x_i \cdot y_i & \sum_{i=1}^{n} y_i^2 & \sum_{i=1}^{n} x_i \cdot y_i^2 & \sum_{i=1}^{n} x_i^2 \cdot y_i & .. & .. & \sum_{i=1}^{n} y_i^{m+1} \\ \sum_{i=1}^{n} x_i \cdot y_i & \sum_{i=1}^{n} x_i^2 \cdot y_i & \sum_{i=1}^{n} x_i \cdot y_i^2 & \sum_{i=1}^{n} x_i^2 \cdot y_i^2 & \sum_{i=1}^{n} x_i^3 \cdot y_i & .. & .. & \sum_{i=1}^{n} x_i \cdot y_i^{m+1} \\ \sum_{i=1}^{n} x_i^2 & \sum_{i=1}^{n} x_i^3 & \sum_{i=1}^{n} x_i^2 \cdot y_i & \sum_{i=1}^{n} x_i^3 \cdot y_i & \sum_{i=1}^{n} x_i^4 & .. & .. & \sum_{i=1}^{n} x_i^2 \cdot y_i^m \\ : & : & : & : & : & .. & .. & : \\ : & : & : & : & : & .. & .. & .. \\ \sum_{i=1}^{n} y_i^m & \sum_{i=1}^{n} x_i \cdot y_i^m & \sum_{i=1}^{n} y_i^{m+1} & \sum_{i=1}^{n} x_i \cdot y_i^{m+1} & \sum_{i=1}^{n} x_i^2 \cdot y_i^m & .. & .. & \sum_{i=1}^{n} y_i^{2.m} \end{bmatrix} \cdot \begin{Bmatrix} \alpha_0 \\ \alpha_1 \\ \alpha_2 \\ \alpha_3 \\ \alpha_4 \\ : \\ : \\ \alpha_{\left(\frac{(m+1(m+2}{2}\right)-1} \end{Bmatrix} = \begin{Bmatrix} \sum_{i=1}^{n} \bar{\eta}(x,y)_i \\ \sum_{i=1}^{n} \bar{\eta}(x,y)_i \cdot x_i \\ \sum_{i=1}^{n} \bar{\eta}(x,y)_i \cdot y_i \\ \sum_{i=1}^{n} \bar{\eta}(x,y)_i \cdot x_i \cdot y_i \\ \sum_{i=1}^{n} \bar{\eta}(x,y)_i \cdot x_i^2 \\ : \\ : \\ \sum_{i=1}^{n} \bar{\eta}(x,y)_i \cdot y_i^m \end{Bmatrix} \quad (12)$$

As such, it is desirable to approximate $\eta(x, y)$, with $(x, y) \in \Omega$ (Fig. 3); in other words, $\eta(x, y)$ is defined in a closed interval of continuous and real vectorial space, using completely orthonormal bases to represent polynomial P_m so that:

$$\eta(x,y) \cong \alpha_0 + \alpha_1 \cdot x + \alpha_2 \cdot y + \alpha_3 \cdot x \cdot y + .. + \alpha_{\left[\frac{(m+1)(m+2)}{2}\right]-1} \cdot y^m = P_m(x,y) \quad (8)$$

and furthermore such that the distances between the points of $\eta(x, y)$ are the closest to the adopted function $P_m(x, y)$, where m is the maximum power of the polynomial.

To determine the polynomial $P_m(x, y)$, the real coefficients should guarantee that:

$$\text{dist}(\eta, P_m) = \text{minimun} \quad (9)$$

The definitions for distance are given by:

$$Q = \text{dist}(\eta, P_m) = \|\eta - P_m\|^2 \quad (10)$$

with

$$Q = \text{dist}(\eta, P_m) = (\eta - P_m, \eta - P_m) = \sum_{k=0}^{n} \left[(\eta(x,y)_k - P_m(x,y)_k\right]^2 \quad (11)$$

and where $(\cdot, \cdot)$ represents the inner product, $\bar{\eta}(x, y)_k$ are the known displacements or bending moments at point k of the

Considering a grid automatic generation applied over the entire domain with a total number of internal points (n), the linear system, Eq. (12), is obtained and it can be solved where unknown values α_i are the polynomial coefficients of each influence surface.

The errors involved in the least square fitting can be estimated by the following expression:

$$\text{Error} = \|\eta - P_m\|^2 = \sum_{k=0}^{n} \left[(\bar{\eta}(x,y)_k - \eta(x,y)_k\right]^2 \quad (13)$$

3.2 Load effect determination

When the influence surfaces are obtained, it is possible to calculate the effect of any load by using the hypothesis that there is a linear superposition of effects.

Hence, the final effect (bending moments or displacements) at a section (s) under a certain load distribution is written as:

$$E_S = \sum_{k=1}^{nc} \left[\eta_s(x_k, y_k) \cdot F_k\right] + \sum_{k=1}^{nd} \left[\int_{\Omega_k} \eta_s(x,y) \cdot q_k(x,y) d\Omega_k\right] \quad (14)$$

where nc and nd are, respectively, the number of concentrated (F) and distributed (q) forces acting on the plate.

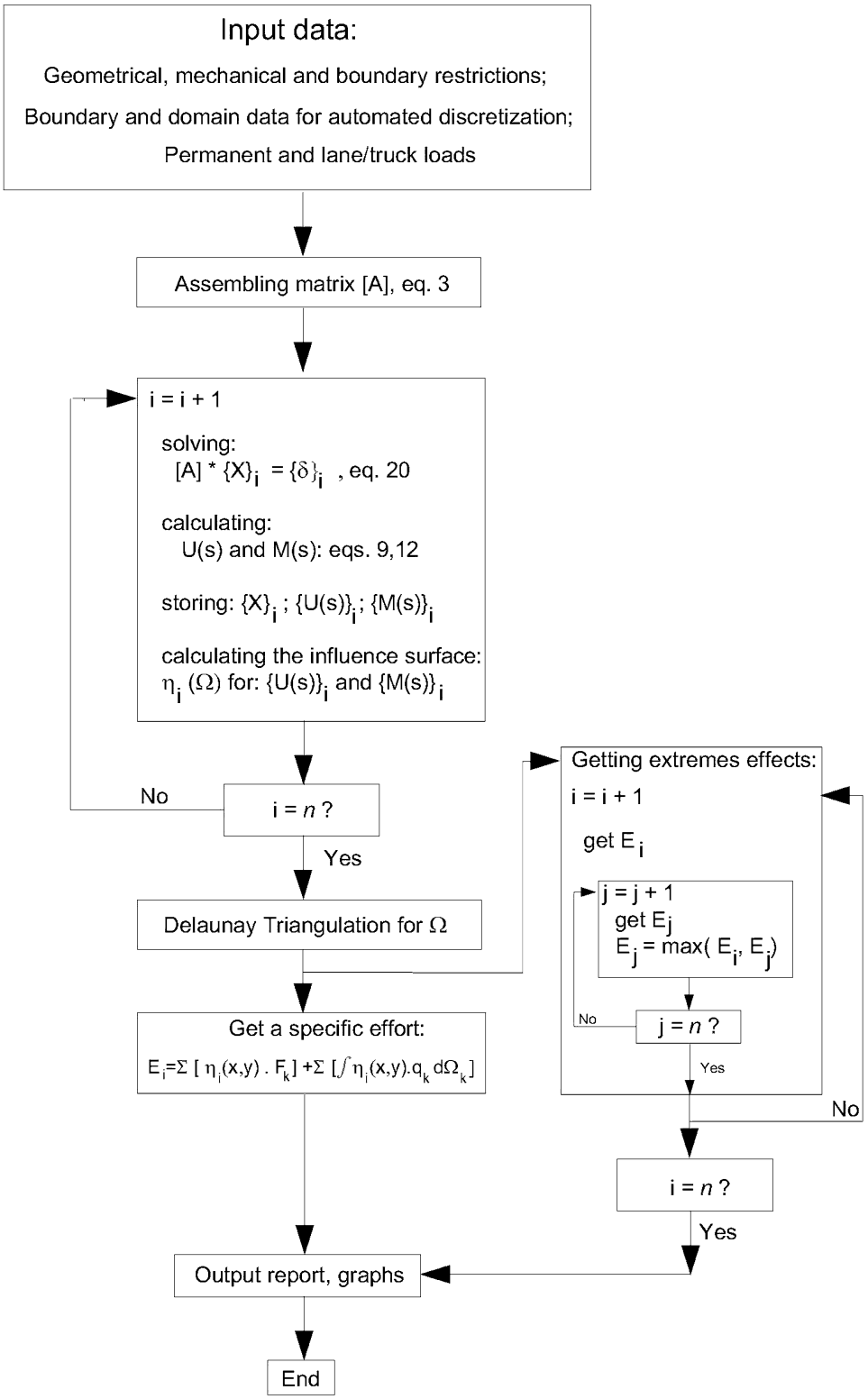

Fig. 5 Flowchart of the computational process

These actions are generated by dead loadings due to structural and non-structural part of bridges and imposed traffic loading due to road vehicles, which are defined by specific codes, for example, AASHTO [1].

In the second part of expression (14), the *k-th* portion referring to the distributed load is numerically integrated over domain Ω_k, which is automatically discretized in triangular elements using the Delaunay triangulation algorithm,

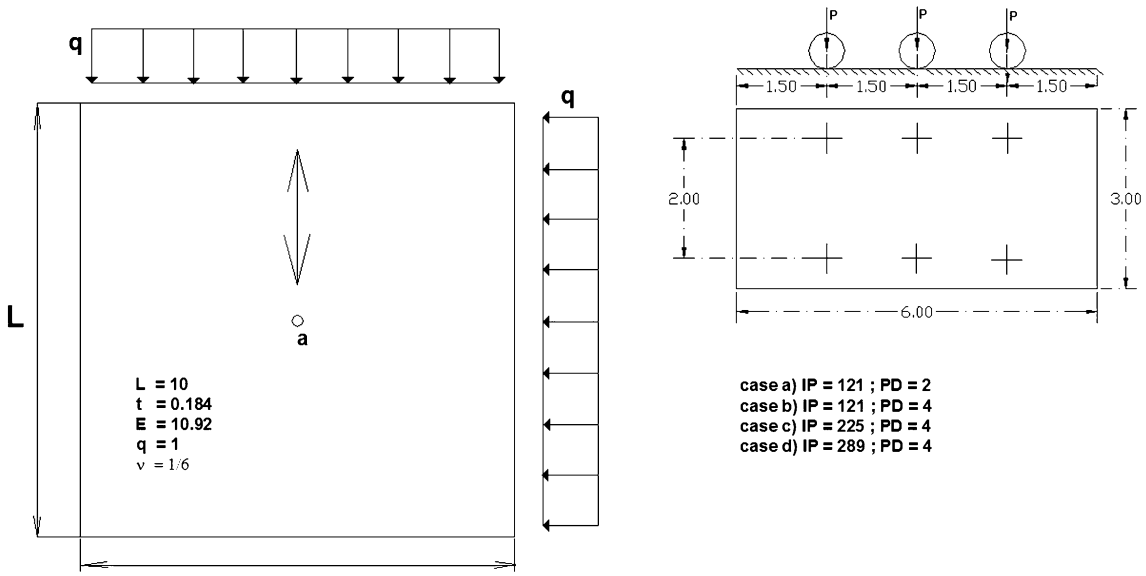

Fig. 6 **a** Geometry, plate data; **b** number of internal points (IP) and polynomial degree (PD); **c** characteristic loads of [10] (1985) including the figure of the vehicular moving loads (*bottom*); **d** propagation of the wheel load from the upper to the middle surface of the plate

Table 1 Transverse displacements and bending moments m_x and m_y at section a

Case	Transversal displacement $w \cdot D/(q \cdot L^4)$	Error (%)	Bending moments $m_x = m_y = m/(q \cdot L^2)$	Error (%)	Time (s)*
a	0.003878	−4.5	0.05173	8.0	57
b	0.004085	0.6	0.05160	7.7	58
c	0.004066	0.1	0.04908	2.4	164
d	0.004063	0.0	0.04852	1.3	257
[21]	0.004062	–	0.04789	–	–

* Intel Core2 Quad CPU/2.83 GHz, 4 GB RAM

the procedure of which was incorporated to the present formulation following Lee and Schachter [19] algorithms. Figure 4 shows a portion of the volume integration to be computed for considering the distributed forces, which is carried out numerically using triangular coordinates, as indicated in Hammer et al. [13] as:

$$E_S^k = \sum_{j=1}^{elem} |J|_j \cdot \left[\sum_{i=1}^{nh} \eta_s(\xi_1^i, \xi_2^i, \xi_3^i) \cdot q_k \cdot w_i \right] \tag{15}$$

where nh is the number of integration points, ξ_1^i, ξ_2^i and ξ_3^i are the homogeneous coordinates of the triangle, J is the Jacobean of element j, and w_i represents the weight factor at the point of integration.

Figure 5 depicts the flowchart of the computational process, but Eq. 3 is replaced with:

$$[A]\{X\}_i = \{\delta\}_i \tag{16}$$

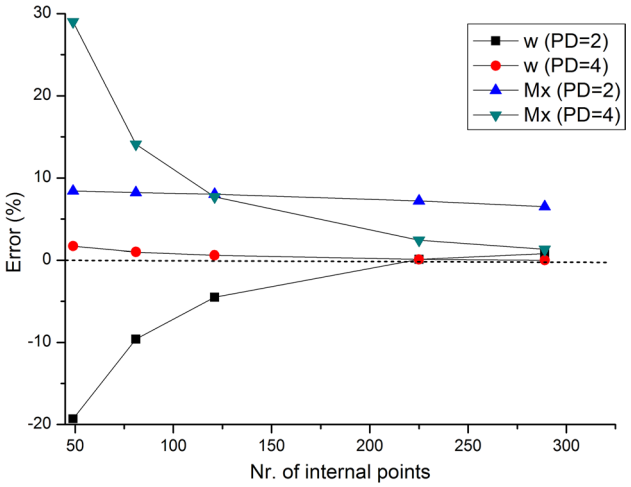

Fig. 7 Convergence of transverse displacements and bending moments on the central plate using the influence surface model

where index i refers to the set of values obtained for the i-th internal point which represents each section (c). The vector on the right side of Eq. (16) represents a function similar to the Kronecker's delta, but with only a unitary value on the vertical position acting at each i-th internal node.

The application of a fundamental solution, or Green function, does not directly provide a defined effect from the application of Eq. (14). This equation represents the computation of the integral whose kernel results from the multiplication of influence surface values with the set of traffic load, concentrated and distributed loads. However, the physical quantity values are obtained punctually at all internal points. Hence, to calculate the integral with distributed loads (Eq. 14), it is necessary to determine a surface which represents the set of these punctual values and the representation must be adjusted by a function for each quantity kind. The adjust function minimizes the approximation errors and, then, analytical surfaces are generated, obtained in this proposal by the least square method; both types of surfaces are here called "extreme quantity surfaces" and "influence surfaces".

4 Numerical example

4.1 Square plate simply supported at the boundaries

The plate in Fig. 6a was discretized into 48 boundary elements and the number of internal points (IP) and the polynomial degree (PD) are also indicated cases in Fig. 6b.

Table 2 Numerical and analytical maximum bending moments (48 elements)

Case	m_x	Error (%)	m_y	Error (%)
IP = 121; PD = 4	104.06	8.1	103.47	10.96
IP = 169; PD = 4	100.93	4.9	100.26	7.5
IP = 441; PD = 4	96.96	0.8	96.13	3.1
Analytical solution, [3]	96.25	–	93.25	–

Equivalent unit concentrated loads were applied to each IP and the effects were calculated using Eqs. (3), (4) and (7) and the relationships (8) and (12), with the 13 integration points mentioned in (1974).

In the present formulation, displacements, bending moments and shear forces at any point in the domain can be obtained. Table 1 presents the results and the processing time necessary to obtain the effects acting on section a, comparing with the plate under only a uniform distributed load. The analytical values are found in Timoshenko [39] and they are: $w \cdot D/(q \cdot L^4) = 0.004062, \quad m_x/(q \cdot L^2) = 0.04789$, with $D = \frac{E \cdot t^3}{12(1-\nu^2)}$.

Figure 7 presents the convergence of transverse displacements and bending moments at the central plate using influence surface model varying the number of the internal points and the polynomial degree.

This simple example aims to evaluate the computational formulation by comparing the present formulation with the analytical solution varying the number of internal points in conjunction with the number of the polynomial degree. Table 1 and Fig. 7 show good accuracy between both different formulations. It is worth pointing out that the present formulation can simulate this classical problem properly.

Pucher [28] presents tables, based on the analytical procedure to calculate influence surfaces on elastic plates. The extreme bending moments in bridge decks subjected to traffic loads are proposed in the German standard [10].

A standard vehicle load is defined to represent all the set of bridge loads, a principal vehicle compounded by six concentrated loads and small vehicles and pedestrians as uniformly distributed loads (Fig. 6c). The principal vehicle is located in a critical position aiming at extreme values of bending moments and the secondary loads distributed in a wide area of the bridge deck. Charts in Pucher [28] are used to calculate the bending moment values following the plate geometry, boundary conditions and mechanical properties of the structural material (Fig. 6a). It is necessary to obtain the wheel contact area, adopting 0.5 m width

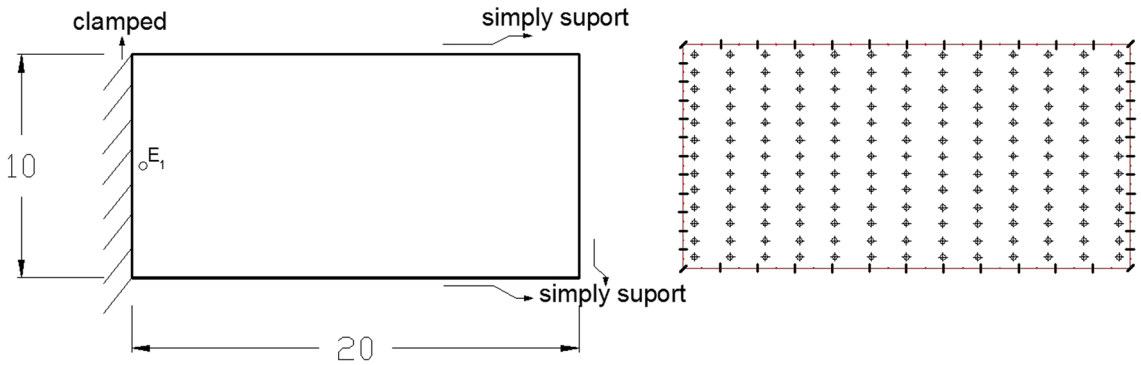

Fig. 8 Geometry, boundary elements and internal points

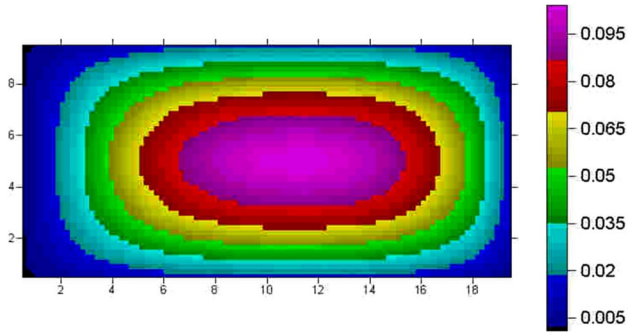

Fig. 9 Maximum transverse displacements w for a moving unit force

and 0.2 m long. The propagation of the wheel load from the upper to the middle surface of the plate is equal to 0.5 m, as can be seen in Fig. 6d.

Following the expressions and chart number 79 presented in Pucher [28], it is possible to obtain the maximum bending moments using the expression:

$$M_{\max} = M_g + M_q = k \cdot g \cdot l^2 + \phi \cdot \left[P \cdot M_L + p \cdot M_p + p' \cdot M_{p'}\right]$$

Adopting in the main lane a distributed dead load $g = 10$ kN/m^2 and null values for the uniformly distributed secondary loads ($p = 0$, front and behind; $p' = 0$, lateral; Fig. 6c), axle loads $p = 75$ kN (standard vehicle class 45), the impact factor is $\phi = 1$, the parameters k, M_{L}, M_{p} and $M_{\mathrm{p'}}$ are obtained using the cited charts.

In Table 2, the analytical values obtained by the charts indicated in Pucher [28] and the ones generated by the present procedure are presented, and the good accuracy between them can be verified. It is worth pointing out the limitation of the geometry and the standard vehicle load that can be considered in the classical charts [28], which is not a drawback for the present formulation, which is general in both aspects, geometric and loads properties.

4.2 Rectangular plate simply supported at 3 boundaries and clamped at 1 boundary (dir. y)

The rectangular plate is simulated with ratio of border dimension $L_x = 2 \cdot L_y$, Fig. 8. The discretization is used for the plate with 48 boundary elements, 169 internal points and polynomial degree 4. Figures 9, 10, 11 show extreme values for displacements and bending moments, by applying the equivalent unitary loading. The material properties are:

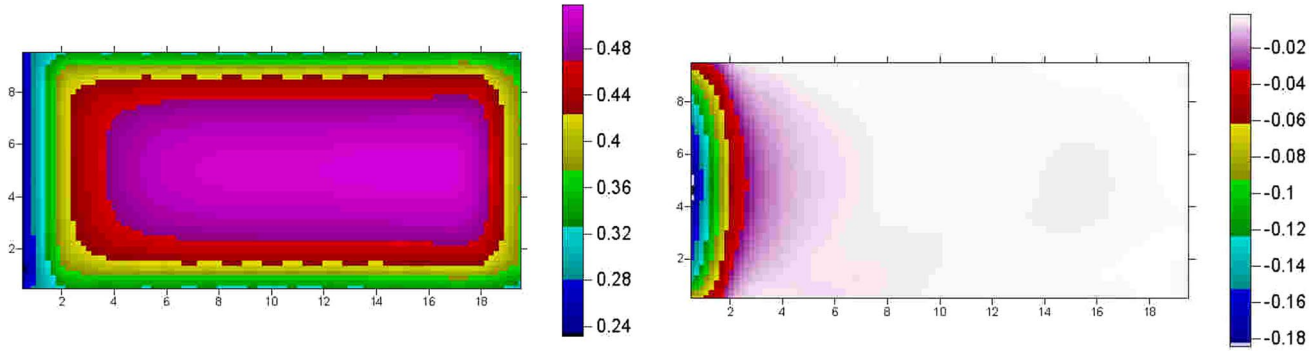

Fig. 10 Maximum/Minimum extreme bending moments m_x for a moving unit force

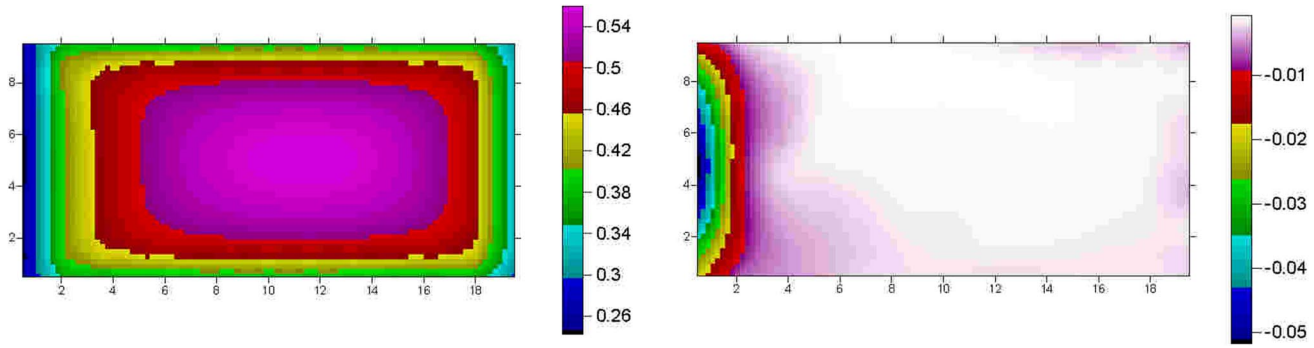

Fig. 11 Maximum/Minimum extreme bending moments m_y for a moving unit force

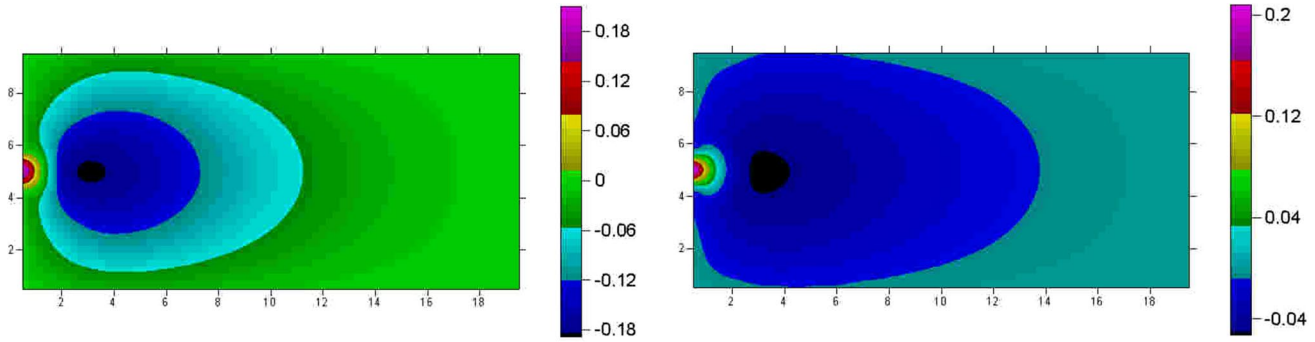

Fig. 12 Influence surface for m_x and m_y in section E_1

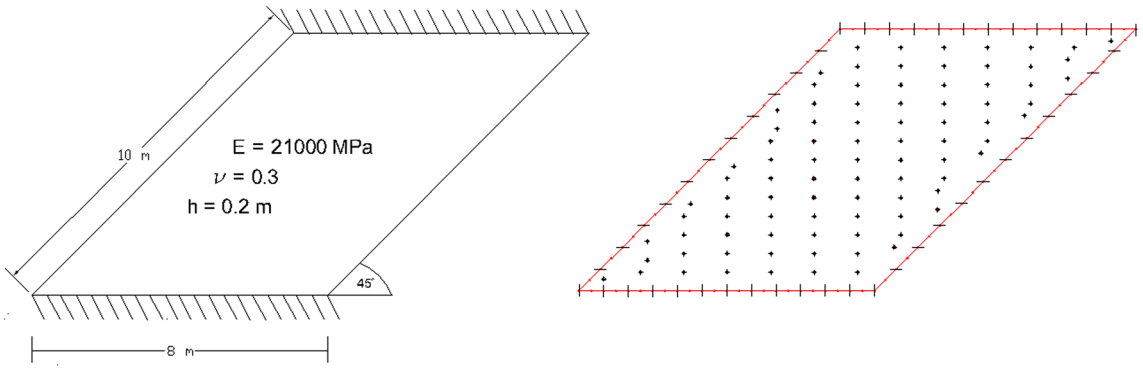

Fig. 13 Geometry, boundary elements and 194 internal points

Young's modulus $E = 21{,}000$ MPa, Poisson's ratio $\nu = 0.3$ and thickness $h = 0.2$ m.

The results of extreme transverse displacements in the plate can be seen in Fig. 9, in which maximum values are noticed to be obtained along the central area. Bending moments m_x in Fig. 10 and m_y in Fig. 11 have the maximum positive values spread over a wide range, covering practically the entire width of the plate area and the minimum negative values very close the clamped boundary.

The graphs presented in Figs. 10 and 11 are not the nominated influence surfaces but surfaces which represent the extreme effects in the plate area for each unitary load position (extreme quantity surfaces). The influence surfaces represent the effects in a specific cross section of the structural element for each unitary load position.

The influence surfaces were evaluated to bending moments m_x and m_y in internal point E_1 (Fig. 8), and the results are, respectively, shown in Fig. 12a, b. The difference between extreme quantity surfaces and the influence surfaces can be observed, for example, by comparing the respective representations for bending moments m_x in Figs. 10 and 12a, respectively. Extreme quantity surfaces represent extreme m_x values in all the internal points of the plate, positive values in all the plate area (Fig. 10a) and negative values close to the clamped boundary (Fig. 10b). The influence surface represents m_x and m_y values (Fig. 12a) in a specific section. In other words, loads positioned over the blue area imply extreme negative values in section E_1.

4.3 Skewed plate (deck) supported at 2 opposite boundaries and free at the 2 other boundaries

Next, two examples show several plate shapes, mainly bridge slabs, simulated by this computational code. Both are modeled assuming Young's modulus $E = 21{,}000$ MPa, Poisson's ratio $\nu = 0.3$ and thickness $h = 0.2$ m.

Now, a skewed plate is simulated, where the plate was divided into 48 boundary elements and 194 internal points and the geometrical and the mechanical parameters are indicated in Fig. 13. The extreme quantity surfaces of transverse displacements and moments (bending m_x, m_y and twisting m_{xy}) are shown in Figs. 14, 15, 16. Figure 14a shows the displacement and Fig. 4b shows the twisting moment m_{xy} values with orders of magnitude from 0.1 to 0.2. The maximum values for m_x and m_y, for a unitary force, are indicated in Figs. 15a and 16a, respectively,

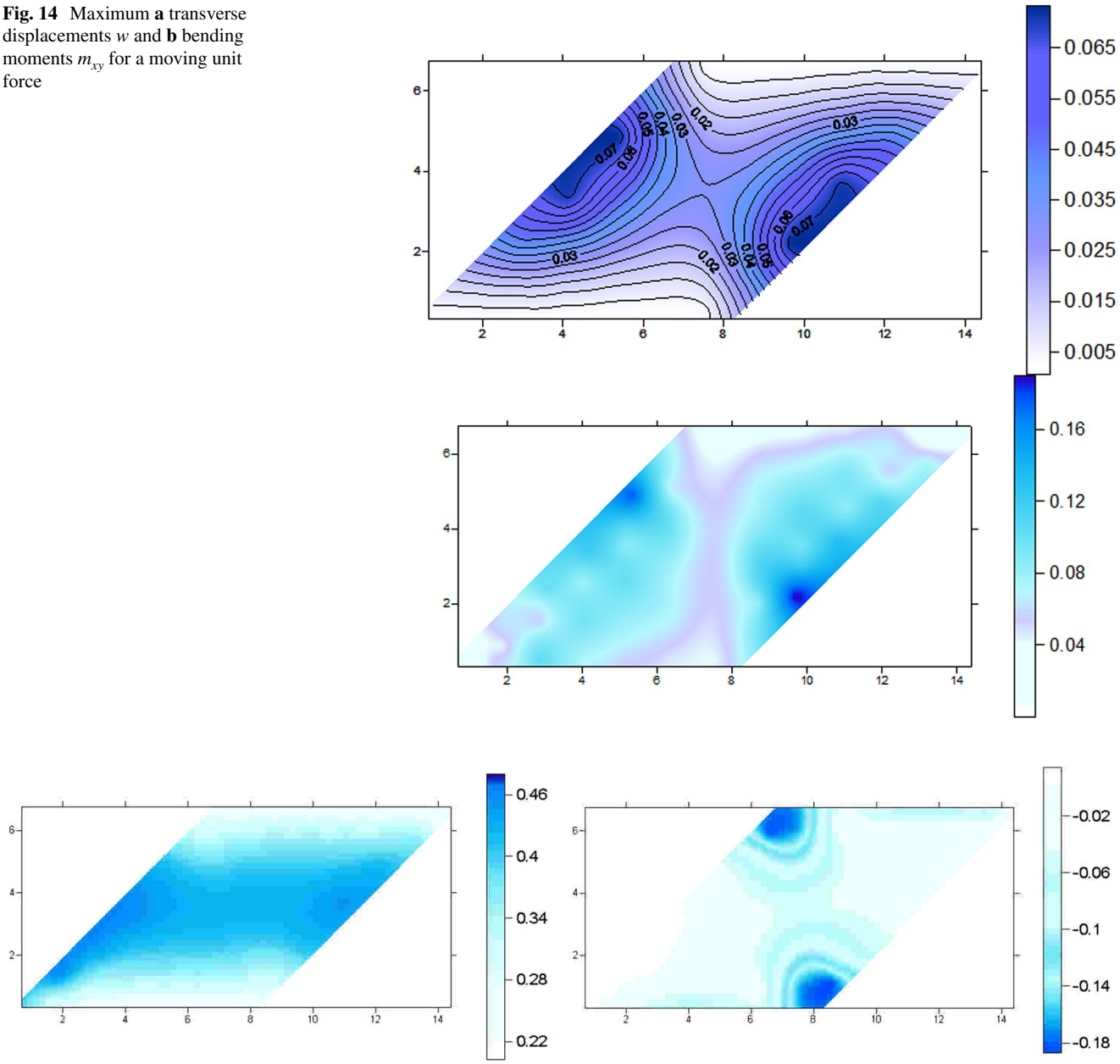

Fig. 14 Maximum **a** transverse displacements w and **b** bending moments m_{xy} for a moving unit force

Fig. 15 Maximum/Minimum extreme bending moments m_x for a moving unit force

spread *boundaries* in the central region of the plate. Likewise, the minimum values for m_x and m_y are indicated in Figs. 15b and 16b, respectively, concentrated near the clamped boundaries. Those values reach magnitudes in the order from 0.3 to 0.6. It also shows the importance of influence surfaces, mainly when partial and/or traffic vehicle loads are presented in plate structures. For the case of reinforced concrete slabs, it is necessary to place additional reinforced bars in the regions with maximum m_{xy}, such as a reinforced mesh armor at 45° to the main orthogonal mesh.

4.4 Circular sector plate clamped at two opposite boundaries and free at two curved boundaries

Simulating a circular sector plate, this problem was divided into 30 boundary elements and 112 internal points. The geometry and the mechanical parameters are indicated in Fig. 17. The extreme quantity surfaces of transverse displacements and moments (bending m_x, m_y) are shown in Figs. 18 and 19. Figure 19 shows the bending moment negative values with an order of magnitude of −30. Negative

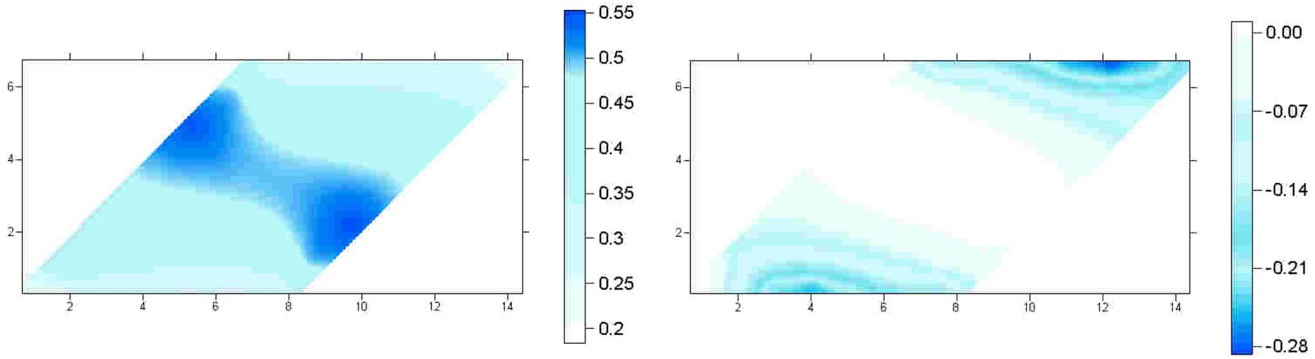

Fig. 16 Maximum/Minimum extreme bending moments m_y for a moving unit force

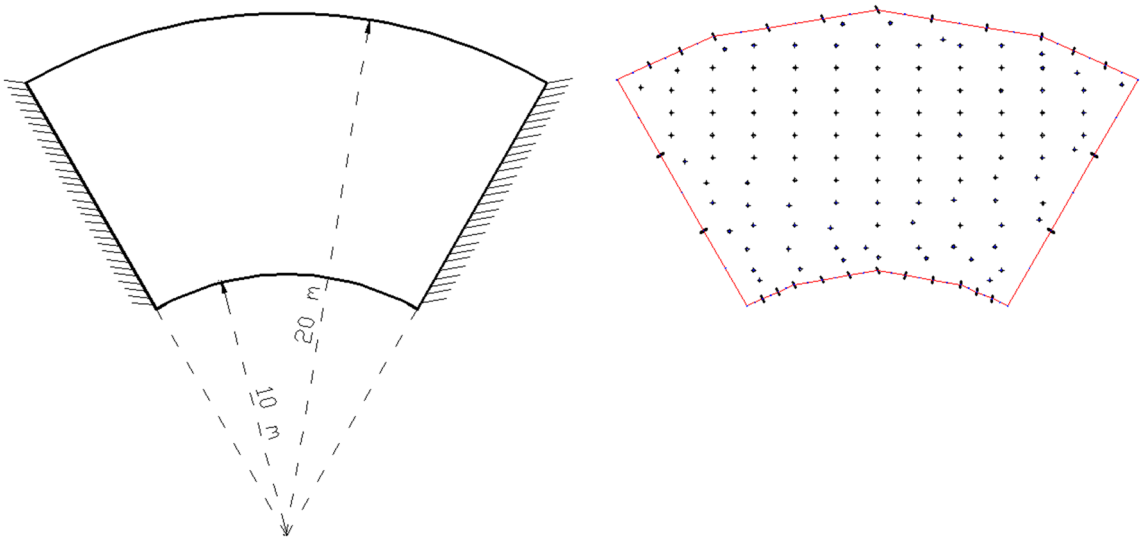

Fig. 17 Geometry, boundary elements and internal points

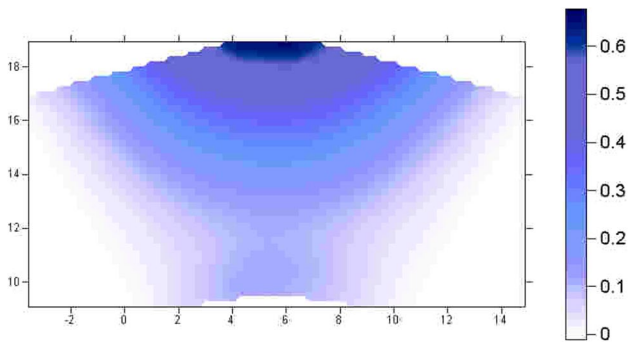

Fig. 18 Maximum transverse displacements w for a moving unit force

values for bending moments occur along external curved free boundary, which means that for a partial load located near this edge, this region will present great negative moment values. In the opposite (internal) curved edge, the envelopes show that a partial load located near this edge do not cause significant bending moments to the plate. It again shows the importance of influence surfaces to determine the regions which, when loaded, will submit the plate with high level of effects, mainly when partial loads are presen ted.

5 Conclusions

In this application, the objective was to use the advantages of BEM to elaborate a useful tool for structural engineers to determine influence surfaces for bending plates. The present formulation allowed eliminating the use of manual charts, which have so far been used for the same purpose, that is, for calculating influence surface of bridge decks, or eliminating the use of FEM software. But both procedures

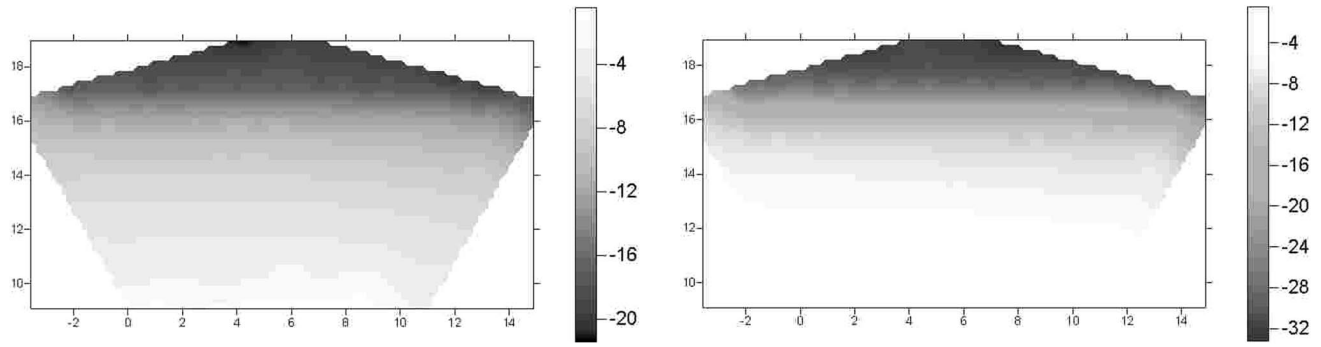

Fig. 19 Minimum extreme bending moments m_x and m_y

have some disadvantage for treating influence surface; the former ones are limited for general problems; the latter requires refining the discretization of the structure geometry to simulate complex problems, which demands huge computational work and the results present strong mesh dependencies.

The present formulation has general characteristics as it permits the simulation of plates with different shapes, including those with curved or circular boundaries, and type of vehicular loads. Manual charts only compute restricted and specific geometry, axle locations and number of wheels, not permitting specified classes or abnormal vehicle loads. The influence surfaces were used to obtain the maximum effects for several loads on the plate. According to the examples formulated by the authors, the present formulation proved to be efficient and robust with a short processing time considering the polynomial power for the computation of the final effect.

Some propositions are implemented to improve the numerical results, as demonstrated in Oliveira Neto and Paiva [21], such as using quadratic functions, a Gaussian coordinate transformation over the boundary elements and the concentrated equivalent shear forces V_n. These propositions also make possible to obtain internal values at points very close to the boundary or to concentrated loads with good numerical precision.

Another important proposition is the approach which considers an equivalent unit concentrated load as a uniformly distributed load over a square region centered by the load point. Domain integrals Ω_g are calculated as a summation of integrals over boundary Γ_g of their respective load region. This proposal avoids the calculation of bending moments at load points with strong singularities in fundamental solutions and high gradients.

Our intention is to present a proposal that demonstrates the methodology for calculation procedures. Equation (14) represents the computation of the maximum effects as an integral with kernel results from the multiplication of influence surface values with the set of vehicular load, concentrated and distributed loads. Analytical surfaces are generated, obtained in this proposal by the least square method, approximating the set of punctual values of physical quantities and it is adjusted to minimize the approximation errors. Two types of surfaces can be generated, here called "extreme quantity surfaces" and "influence surfaces".

Another research will be conducted to amplify its usage and prove it in comparison against charts. One of the future objectives will be applications in building floor or bridge slabs that are supported on flexible beams, over columns or pavements with potholes, through optimization techniques, in which the critical regions can be pinpointed, such as vehicle-type traffic.

Acknowledgments The authors thank the Department of Structural and Foundation Engineering, School of Engineering of the University of São Paulo (EPUSP) for the financial support to this research.

References

1. AASHTO (1983) Standard specifications for highway bridges, 13th edn. AASHTO, Washington
2. Abdel-akher A, Hartley GA (1989) Evaluation of boundary integrals for plate bending. Int J Num Meth Eng 28(2):75–93. doi:10.1002/nme.1620280107)
3. Almeida VS, Paiva JB (2004) A mixed BEM-FEM formulation for layered soil-superstructure interaction. Eng Anal Bound Elem 28:1111–1121
4. Almeida VS, Paiva JB (2007) Static analysis of soil/pile interaction in layered soil by BEM/BEM coupling. Adv Eng Softw 38:835–845
5. Beskos DE (1991) Boundary element analysis of plates and shells. Springer, Berlin
6. Bezine G (1978) Boundary integral formulation for plate flexure with arbitrary boundary conditions. Mech Res Commun 5(4):197–206
7. Botta AS, Venturini WS, Benallal A (2005) BEM applied to damage models emphasizing localization and associated regularization techniques. Eng Anal Bound Elem 29:814–827
8. Citarella R, Cricrì G (2009) A two-parameter model for crack growth simulation by combined FEM-DBEM approach. Adv Eng Softw 40(5):363–377

9. Citarella R, Cricrì G (2010) Comparison of DBEM and FEM crack path predictions in a notched shaft under torsion. Eng Fract Mech 77(11):1730–1749
10. DIN (1072) Straßen und Wegbrücken. Lastannahmen, Dezember **1985**
11. Fernandes GR (2009) A BEM formulation for linear bending analysis of plates reinforced by beams considering different materials. Eng Anal Bound Elem 33(8–9):1132–1140
12. Fudoli CA, Benallal A, Venturini WS (2002) An implicit BEM formulation for gradient plasticity and localization phenomena. Int J Num Meth Eng 53:1853–1869
13. Hammer PC, Marlowe OJ, Stroud AH (1956) Numerical integration over simplexes and cones. Math Tables Other Aids Comput 10:130–137
14. Hansen EB (1976) Numerical solution of integro-differential and singular integral equations for plate bending problems. J Elast 6(1):39–56
15. Hartmann F, Zotemantel R (1986) The direct boundary element method in plate bending. Int J Num Meth Eng 23(11):2049–2069
16. Hwu Ch (2012) Boundary element formulation for the coupled stretching–bending analysis of thin laminated plates. Eng Anal Bound Elem 36(6):1027–1039
17. Kong J (2009) A practical method to determine critical moments of bridge decks using the method of least squares and spreadsheets. In: Yuan Y, Cui J, Mang HA (Eds.) Proceedings of the international symposium on computational structural engineering, held in Shanghai, China, June 22–24
18. Lawson C, Hanson R (1974) Solving least squares problems. Prentice-Hall, Englewood Cliffs
19. Lee DT, Schachter BJ (1980) Two algorithms for construction ga Delaunay triangulation. Int J Comput Inform Sci 9(3):219–242
20. Memari AM, West HH (1991) Computation of bridge design forces from influence surfaces. Comput Struct 38(5/6):547–556
21. Oliveira Neto L, Paiva JB (1993) Analysis of curved plates by the Boundary Element Method. Eng Anal Bound Elem 12:57–64
22. Oliveira Neto L, Paiva JB (2003) A special BEM for elastostatic analysis of building floor slabs on columns. Comput Struct 81(6):359–372
23. Orakdogan E, Girgin KM (2005) A direct determination of influence lines and surfaces by FEM. Struct Eng Mech 20(3):279–292
24. Paiva JB, Venturini WS (1987) Analysis of building structures considering plate-beam-column interactions. In: Brebbia CA, Venturini WS (eds.), Boundary element techniques, CML Publ., Southampton
25. Paiva WP, Sollero P, Albuquerque EL (2011) Modal analysis of anisotropic plates using the boundary element method. Eng Anal Bound Elem 35(12):1248–1255
26. Palermo L Jr (2012) The tangential differential operator applied to a stress boundary integral equation for plate bending including the shear deformation effect. Eng Anal Bound Elem 36(8):1213–1225
27. Paris F, Leon S (1986) Simply supported plates by boundary integral equation method. Int J Num Meth Eng 23:173–191
28. Pucher A (1977) Influence surfaces of elastic plates. Springer, New York
29. Rashed YF (2008) A relative quantity integral equation formulation for evaluation of boundary stress resultants in shear deformable plate bending problems. Eng Anal Bound Elem 32(2):152–161
30. Rusch H, Hergenroder A (1964) Influence surfaces for moments in skew slabs. (Translation from the German). Cement and Concrete Association
31. Rusch EH (1965) Berechnungstafeln fur rechtwinklige Fahrbahnplatten von Strabenbrucken. Verlag von Wilhelm Ernst & Sohn, Berlin
32. Sapountzakis EJ, Mokos VG (2008) An improved model for the analysis of plates stiffened by parallel beams with deformable connection. Comput Struct 86(23–24):2166–2181
33. Shao W, Wu X (2011) Fourier differential quadrature method for irregular thin plate bending problems on Winkler foundation. Eng Anal Bound Elem 35(3):389–394
34. Shen W (1992) The generalized Muller-Breslau principle for higher-order elements. Comput Struct 44:207–212
35. Song GS, Mukherjee S (1986) Boundary element method analysis of bending of elastic plates of arbitrary shape with general boundary conditions. Eng Anal 3(1):36–44
36. Stern MA (1979) General boundary integral formulation for the numerical solution of plate bending problems. Int J Solids Struct 15:769–782
37. Tan F, Zhang YL (2013) The regular hybrid boundary node method in the analysis of thin plate structures subjected to a concentrated load. Eur J Mech A/Solids 38:79–89
38. Tan F, Zhang YL, Wang YH (2011) A meshless hybrid boundary node method for Kirchhoff plate bending problems. CMES Comput Model Eng Sci 75(1):1–31
39. Timoshenko S (1940) Theory of plates and shells. Mcgraw-Hill, New York
40. Tottenham H (1979) The boundary element method for plates and shells. In: Banerjee PK, Butterfield R (eds) Developments boundary element methods 1. Applied Science Publ, London, pp 173–205
41. Waidemam L, Venturini WS (2009) An extended BEM formulation for plates reinforced by rectangular beams. Eng Anal Bound Elem 33(7):983–992
42. Wu BC, Altiero NJ (1979) A boundary integral method applied to plates of arbitrary plan form and arbitrary boundary conditions. Comput Struct 10:703–707
43. Xia P, Long SY, Cui HX, Li GY (2009) The static and free vibration analysis of a nonhomogeneous moderately thick plate using the meshless local radial point interpolation method. Eng Anal Bound Elem 33(6):770–777